Spin-density-functional theory of circular and elliptical quantum dots

Kenji Hirose* and Ned S. Wingreen
NEC Research Institute, 4 Independence Way, Princeton, New Jersey 08540
(Received 14 August 1998)

Using spin-density-functional theory, we study the electronic states of a two-dimensional parabolic quantum dot with up to $N=58$ electrons. We observe a shell structure for the filling of the dot with electrons. Hund's rule determines the spin configuration of the ground state, but only up to 22 electrons. At specific N, the ground state is degenerate, and a small elliptical deformation of the external potential induces a rotational charge-density-wave state. Previously identified spin-density-wave states are shown to be artifacts of broken spin symmetry in density-functional theory. [S0163-1829(99)03507-9]

Quantum dots have recently attracted much interest both experimentally and theoretically. One realization of a quantum dot is a small island fabricated in a two-dimensional electron gas laterally confined by an external potential and containing a few to a few hundred electrons.[1] Experimentally, measuring the tunnel conductance[2] and capacitance[3] by changing the gate voltage attached to the quantum dot, one observes a peak every time the average number of electrons increases by 1. The spacing of peaks, or addition spectrum, reflects the energy differences between ground states of the dot with different numbers of electrons. Each disordered dot has its own characteristic addition spectrum, but recently it has become possible to fabricate dots so clean that the addition spectra are reproducible from dot to dot.[4] Among the features of these clean, parabolic dots are atomiclike shell structures, Hund's rules, and reproducible transition rates.[4]

The advent of atomiclike spectra in quantum dots calls for appropriately quantitative theoretical tools. Presently, exact diagonalization of the full Hamiltonian is limited to a small number of electrons in the dot.[5,6] Thomas-Fermi, Hartree,[7] and Hartree-Fock methods[8,9] all suffer from sizeable systematic errors. Here, we treat the electronic states of a dot using the density-functional method[10,11] explicitly including spin.[12–14] We find shell structures in the addition-energy spectrum for a circular, parabolic external potential. Hund's rule determines the ground-state spin configurations, but only up to 22 electrons. Elliptically deforming the external potential eliminates the shell structures, and Hund's rule is replaced by a more Pauli-like behavior of the total spin. At specific N, the ground state is degenerate, and a small elliptical deformation of the external potential induces a rotational charge-density-wave (CDW) state. The spin-density-wave (SDW) states found by Koskinen, Manninen, and Riemann[12] (KMR) are artifacts of broken spin symmetry in density-functional theory.

We solve the following Kohn-Sham equations numerically for a two-dimensional parabolic quantum dot, and iterate until self-consistent solutions are obtained;[15]

$$\left[-\frac{\hbar^2}{2m^*}\nabla^2+\frac{e^2}{\kappa}\int\frac{\rho(\mathbf{r}')}{|\mathbf{r}-\mathbf{r}'|}d\mathbf{r}'+\frac{\delta E_{\rm xc}[\rho,\zeta]}{\delta\rho^{\sigma}(\mathbf{r})}+\frac{1}{2}m^*\omega_0^2r^2\right]\times\Psi_i^{\sigma}(\mathbf{r})=\epsilon_i^{\sigma}\Psi_i^{\sigma}(\mathbf{r}), \tag{1}$$

$$\rho(\mathbf{r})=\sum_{\sigma}\rho^{\sigma}(\mathbf{r})=\sum_{\sigma}\sum_{i}|\Psi_i^{\sigma}(\mathbf{r})|^2. \tag{2}$$

Here σ denotes the spin index, $\zeta(\mathbf{r})$ is the local spin polarization, and $E_{\rm xc}$ is the exchange-correlation energy functional, for which we use the local-density approximation[16]

$$E_{\rm xc}=\int\rho(\mathbf{r})\epsilon_{\rm xc}[\rho(\mathbf{r}),\zeta(\mathbf{r})]d\mathbf{r}, \tag{3}$$

$$\zeta(\mathbf{r})=\frac{\rho^{\uparrow}(\mathbf{r})-\rho^{\downarrow}(\mathbf{r})}{\rho(\mathbf{r})}. \tag{4}$$

To solve the equation, we expand the $\Psi_i^{\sigma}(\mathbf{r})$ in a Fock-Darwin representation;

$$\varphi_{n,k}^{\sigma}(r,\theta)=|n,k\rangle=\sqrt{\frac{n!}{2\pi(n+|k|)!}}\frac{1}{l}\times e^{-r^2/4l^2}\left(\frac{r^2}{2l^2}\right)^{|k|/2}\mathrm{L}_n^{|k|}\left(\frac{r^2}{2l^2}\right)e^{-ik\theta}\chi_{\sigma},$$

where $\mathrm{L}_n^{|k|}(x)$ is a Laguerre polynomial, $l=\sqrt{\hbar/(2m^*\omega_0)}$ and χ_{σ} is a spin function. The noninteracting, single-particle levels form a ladder, $\epsilon_{n,k}=(2n+|k|+1)\hbar\omega_0=M\hbar\omega$, with rung degeneracy M. The ground-state energy of a quantum dot with N electrons is obtained from

$$E(N)=\sum_{i,\sigma}\epsilon_i^{\sigma}-\frac{e^2}{2\kappa}\int\frac{\rho(\mathbf{r})\rho(\mathbf{r}')}{|\mathbf{r}-\mathbf{r}'|}d\mathbf{r}d\mathbf{r}'-\sum_{\sigma}\int\rho^{\sigma}(\mathbf{r})\frac{\delta E_{\rm xc}[\rho,\zeta]}{\delta\rho^{\sigma}(\mathbf{r})}d\mathbf{r}+E_{\rm xc}. \tag{5}$$

We use the material constants for GaAs, $m^*=0.067m$, $\kappa=12.9$, and the external potential is fixed at $\hbar\omega_0=3.0$ meV. The resulting dimensionless interaction strength is $(e^2/\kappa\ell_0)/\hbar\omega_0=1.9$, where $\ell_0=\sqrt{\hbar/(m^*\omega_0)}$.

Shell structure. At low temperatures, electron hopping into a dot containing N electrons is suppressed except when the ground-state energy $E(N)$ is equal to $E(N+1)$. This degeneracy condition determines the observed conductance oscillation peaks that occur at the chemical potentials $\mu(N+1)=E(N+1)-E(N)$. The addition energy $\Delta(N)$ needed

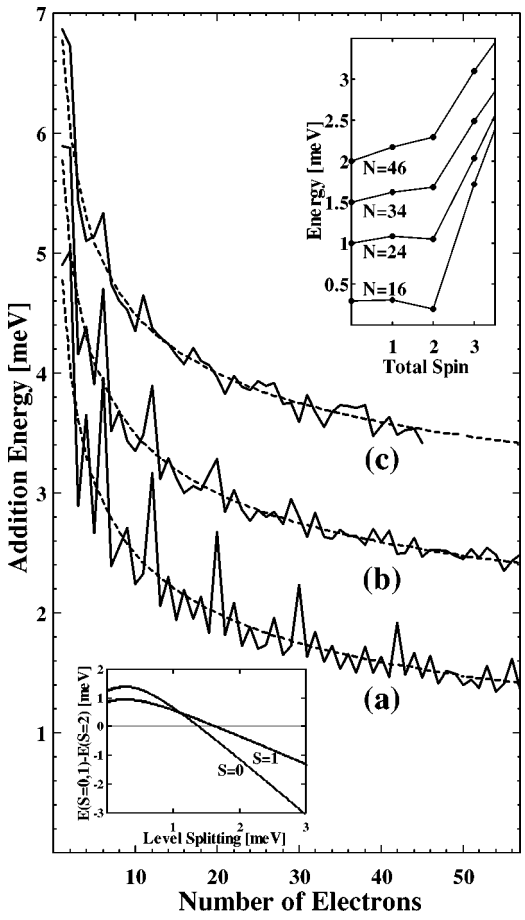

FIG. 1. Addition energy $\Delta(N)$ as a function of electron number N in the dot for (a) a confining parabolic potential $m^*\omega_0^2 r^2/2$ and (b,c) elliptical confining potentials $V(\mathbf{r})=m^*(\omega_x^2 x^2+\omega_y^2 y^2)/2$. The dotted lines indicate the addition energy according to a classical electrostatic analysis (Ref. 17). The parameters are (a) $\hbar\omega_0=3.0$ meV, (b) $\omega_y^2/\omega_x^2=11/13$ and (c) $\omega_y^2/\omega_x^2=5/7$. (b) and (c) are shifted by 1.0 meV and 2.0 meV, respectively. Upper inset—total energy in meV as a function of total spin for electron numbers $N=16$, 24, 34, and 46 in (a). The origin of energy for each N is arbitrary. Lower inset—total energy for $N=4$ electrons obtained by exact diagonalization within a restricted Hilbert space, $|0,\pm 4\rangle$ and $|1,\pm 2\rangle$, as a function of single-particle level splitting Δ. The energies $E(S=0,\ L_z=0)$ and $E(S=1,\ L_z=\pm 2)$ are plotted relative to $E(S=2,\ L_z=0)$.

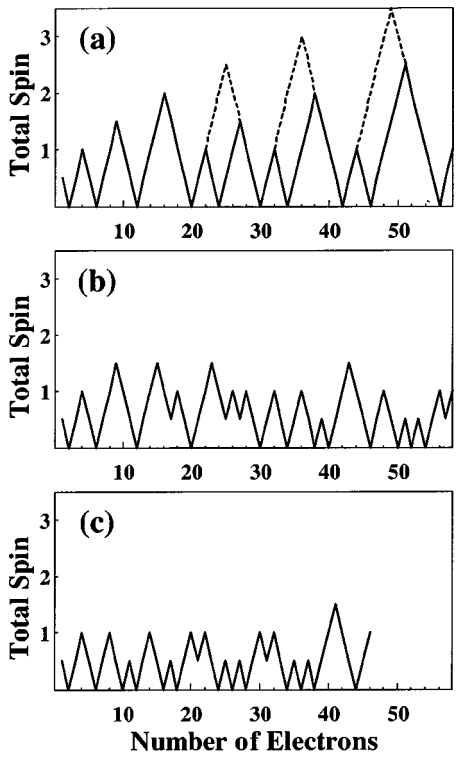

FIG. 2. Ground-state spin as a function of electron number N for (a) the parabolic confining potential and (b,c) the elliptical confining potentials of Fig. 1 The dotted line in (a) indicates the spin configuration when Hund's rule is satisfied.

to put an extra electron in the dot is obtained from $\Delta(N)=\mu(N+1)-\mu(N)=E(N+1)-2E(N)+E(N-1)$. Figure 1(a) shows the addition energy $\Delta(N)$ as a function of electron number N for a circular, parabolic potential. The dotted line indicates $\Delta(N)$ obtained from a classical electrostatic analysis with no kinetic energy.[17] Overall, $\Delta(N)$ decreases with N, as the dot and its capacitance grow. On average, the addition energy obtained from the density-functional calculation is close to the classical electrostatic result e^2/C. However, we see small zig-zag structures, and large peaks at electron numbers $N=2$, 6, 12, 20, 30, 42, and 56. In the single-particle spectrum for a parabolic potential, the electronic states of the dot form closed shell structures at these numbers. Even in the presence of electron-electron interaction, extra energy is required to add one more electron to a closed shell. The peak heights decrease as the number N increases, consistent with recent experiments in which peaks were observed in the addition energy up to 12 electrons.[4]

Hund's rule. By analogy to atoms, we expect that Hund's rule for total spin will apply in the present situation. According to Hund's rule, as degenerate states are filled, the total spin S takes the maximum value allowed by the exclusion principle and becomes zero for closed shells. Figure 2(a) shows the spin configuration as a function of the electron number N for the circular, parabolic potential. The dotted line represents the spin configuration when Hund's rule is satisfied. We can see that, for up to 22 electrons filling the dot, the spin configurations obey Hund's rule.[4] For larger dots, Hund's rule is violated and the high spin states are suppressed. In particular, the total spin becomes zero at electron numbers $N=24$, 34, 46 instead of the expected $S=2$. In the upper inset of Fig. 1, we show the total energy $E(N)$ as a function of the total spin for these states. At $N=16$, the $S=2$ state is 0.10 meV lower in energy than the $S=0$ state, which follows Hund's rule. In contrast, at $N=24$ the $S=0$ state is 0.05 meV lower in energy than the $S=2$ state. This trend is enhanced as the number increases. These energy differences are sufficiently small that weak magnetic fields, of order 300 G, will favor an $S=2$ ground state.

The breakdown of Hund's rule is due to the nonparabolic effective potential caused by Coulomb interactions. For example, without interactions $N=24$ corresponds to 20 electrons in filled inner shells and four ''valence'' electrons distributed among 10 degenerate states: $|n,k\rangle=|0,\pm 4\rangle,|1,\pm 2\rangle$, and $|2,0\rangle$, spin up and down. Coulomb interactions deform the radial potential and lower the energy of the single-particle states with larger angular momentum $|k|$. The

system could minimize its *exchange* energy by creating an $S=2$ state, i.e., putting all four valence electrons into spin up states. Instead, for $N=24$, the system minimizes its *single-particle* energy by putting all four electrons into $k=\pm 4$ states, giving a total spin $S=0$, and breaking Hund's rule.

To confirm this result, we performed an exact diagonalization of $N=4$ valence electrons in a restricted basis set of eight states: $|0,\pm 4\rangle$ and $|1,\pm 2\rangle$, spin up and down. The Hamiltonian we employed is

$$H=\sum_{i=1}^{N=4}\left[-\frac{\hbar^2}{2m^*}\nabla_i^2+\frac{1}{2}m^*\omega_0^2 r_i^2+\gamma r_i^4\right]+\sum_{i<j}\frac{e^2}{\kappa|\mathbf{r}_i-\mathbf{r}_j|}, \tag{6}$$

where the γr_i^4 term is introduced to split the degenerate single-particle energies $\epsilon_{0,\pm 4}$ and $\epsilon_{1,\pm 2}$. The resulting eigenstates of the four electrons can be labeled by total spin S and S_z and total angular momentum L_z. In the lower inset of Fig. 1, we have plotted the total energy as a function of $\Delta=\epsilon_{1,\pm 2}-\epsilon_{0,\pm 4}$. If the splitting Δ is small, the ground state is $S=2$, $L_z=0$, consistent with Hund's rule. But for Δ larger than 1.4 meV, the ground state becomes $S=0$, $L_z=0$, indicating a violation of Hund's rule.

Spin-density-wave states. For a dot with circular symmetry, the eigenstates can always be chosen to have definite angular momentum L_z, and hence circularly symmetric charge density. Nevertheless, Koskinen, Manninen and Reimann[12] reported recently on a spontaneous breaking of circular symmetry in a spin-density-functional calculation of a parabolic quantum dot. Indeed, we confirm that Eqs. (1-5) yield spin-density-wave (SDW) ground states at particular numbers of electrons, e.g., $N=24$, 34, as reported in Ref. 12. These are precisely the $S=0$ ground states discussed above in the context of breaking of Hund's rule. Within spin-density-functional theory, even for $S=0$, the system lowers its exchange energy slightly by mixing in $k=\pm 2$ states with the lower-lying $k=\pm 4$ orbitals. The result is a SDW state. However, from our exact diagonalization studies with $N=4$ in the restricted basis set, we find that the SDW states are due to an unphysical mixture between states of different total spin: $S=0$, $S_z=0$ and $S=1$, $S_z=0$. Hence, the SDW states are artifacts of the well known difficulty of spin-density-functional theory that only the S_z component of total spin can be specified. We conclude that the correct ground states for $N=24$, 34, and 46 have $S=0$, $L_z=0$ and retain circularly symmetry.

Charge-density-wave states. We also find that for certain N (cf. Table I), Equations (1–5) predict a rotational charge-density wave (CDW) near the edge of the dot. Figure 3 shows an example of such a CDW state for $N=31$. The numbers shown in boldface in Table I indicate a strong spin-density modulation, as for $\rho^{\uparrow}(\mathbf{r})$ at $N=31$, while a weaker modulation occurs in the opposite spin density. The numbers in boldface correspond to a closed shell plus one electron, indicating that the extra electron is added to the lowest orbital in the next shell, namely, the one with highest angular momentum. By circular symmetry, this orbital is doubly degenerate. Hence the ground state of the entire dot is doubly degenerate. (In contrast to atoms, the spin-orbit interaction in GaAs dots is too small to split this degeneracy.[18]) The spin-density-functional result is a mixture of these two degenerate ground states. For example, at $N=31$ the total angular momentum will be $L_z=\pm 5$, giving a charge-density modulation $\sim|\exp(i5\theta)+\exp(-i5\theta)|^2\sim\cos^2(5\theta)$ as observed in Fig. 3.

TABLE I. The numbers ($N=N^{\uparrow}+N^{\downarrow}$) of electrons for which spin-density-functional theory predicts a rotational charge-density wave (CDW) near the edge of the quantum dot. The numbers in boldface indicate a strong modulation of the associated spin density, while a weaker modulation occurs in the opposite spin density. The total angular momentum $|L_z|$ of the degenerate pair of ground states giving rise to the CDW is also shown.

Number of Electrons (N)	Spin up ($N^{\uparrow}$)	Spin down ($N^{\downarrow}$)	Total $\lvert Lz\rvert$
3	**2**	1	1
5	3	**2**	1
7	**4**	3	2
10	6	**4**	2
13	**7**	6	3
17	10	**7**	3
21	**11**	10	4
23	12	**11**	4
31	**16**	15	5
33	17	**16**	5
43	**22**	21	6
45	23	**22**	6
57	**29**	28	7

We have investigated the charge density $\rho^{\sigma}(\mathbf{r})$ for $N=3$ by exact diagonalization to confirm the above interpretation. As expected, we find that there are two degenerate ground states, with $L_z=\pm 1$, and that a coherent mixture of these

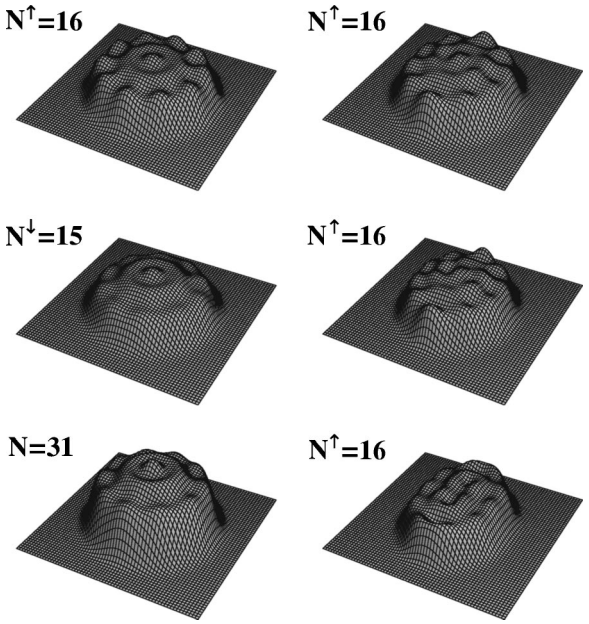

FIG. 3. Charge-density distributions at $N=31$. Left column—from top to bottom, spin-up ($N^{\uparrow}=16$), spin-down ($N^{\downarrow}=15$), and total charge-density distribution. Right column—spin-up charge-density distributions ($N^{\uparrow}=16$) for elliptical potentials, $\omega_y^2/\omega_x^2=11/13$ (top), $\omega_y^2/\omega_x^2=4/5$ (middle), and $\omega_y^2/\omega_x^2=5/7$ (bottom), respectively.

states produces almost exactly the same charge density obtained in the density-functional calculation.

Elliptical dots. To investigate the effect of removing circular symmetry, we consider elliptically deformed potentials $V(\mathbf{r})=m^*(\omega_x^2x^2+\omega_y^2y^2)/2$, with $\omega_0^2=(\omega_x^2+\omega_y^2)/2$, which lift the large degeneracies of the shell structure. Figures 1(b) and 1(c) show that as the deformation grows the regular zigzag pattern found for the circular potential becomes irregular and the large peaks at large N disappear. One can still see large peaks at $N=2$, 6, 12, and 20 electrons in (b), which are the remnants of the closed-shell structures. However, in (c) such large peaks are present only at $N=2$ and 6.

Figures 2(b) and 2(c) show the spin configurations for the same deformed external potentials. We can see that Hund's rule is satisfied up to $N=15$ in (b) but only up to only $N=8$ electrons in (c). The high spin states are suppressed as the deformation becomes significant—the loss of the closed-shell structures results in a more Pauli-like behavior of the total spin.[19]

Figure 3 shows the up-spin densities in deformed potentials for $N=31$, $N^{\uparrow}=16$. We find that true CDW ground states are induced by the increasing elliptical deformation of the external potential. The ground-state spin is $S=1/2$ in all three cases. The charge-density wave has period $\sim\cos^2(5\theta)$ and results from the mixing of the degenerate $L_z=\pm5$ states by the elliptical external potential.

In conclusion, we have studied the electronic states of quantum dots with up to 58 electrons for parabolic circular and elliptical external potentials, using spin-density-functional theory and exact diagonalization. For a circular potential, we observe a shell structure for the filling of the dot with electrons. Hund's rule determines the spin configuration of the ground state up to 22 electrons. For specific numbers of electrons, CDW states appear on small elliptical deformation of the external potential, while previously identified SDW states[12] are found to be artifacts of broken spin symmetry in density-functional theory. For elliptical potentials, the shell structures are lost with increasing deformation, and the spin configurations change from Hund's rule to a more Pauli-like behavior.

We acknowledge O. Agam, I.L. Aleiner, B.L. Altshuler, D.J. Chadi, W. Kohn, Y. Meir, and M. Stopa for comments and suggestions.

*Permanent address: Fundamental Research Laboratories, NEC Corporation, 34 Miyukigaoka, Tsukuba, 305-8501, Japan.

[1] M. A. Kastner, Rev. Mod. Phys. **64**, 849 (1992); R. C. Ashoori, Nature (London) **379**, 413 (1996).

[2] U. Meirav, M. A. Kastner, and S. J. Wind, Phys. Rev. Lett. **65**, 771 (1990).

[3] R. C. Ashoori, H. L. Stormer, J. S. Weiner, L. N. Pfeiffer, S. J. Pearton, K. W. Baldwin, and K. W. West, Phys. Rev. Lett. **68**, 3088 (1992).

[4] S. Tarucha, D. G. Austing, T. Honda, R. J. van der Hage, and L. P. Kouwenhoven, Phys. Rev. Lett. **77**, 3613 (1996); Jpn. J. Appl. Phys., Part 1 **36**, 3917 (1997).

[5] We find good agreement between our results and exact diagonalization results obtained for up to five electrons; P. A. Maksym and T. Chakraborty, Phys. Rev. Lett. **65**, 108 (1990); D. Pfannkuche, V. Gudmundsson, and P. A. Maksym, Phys. Rev. B **47**, 2244 (1993); P. Hawrylak and D. Pfannkuche, Phys. Rev. Lett. **70**, 485 (1993); J. J. Palacios, L. M. Moreno, G. Chiappe, E. Louis, and C. Tejedor, Phys. Rev. B **50**, 5760 (1994).

[6] M. Eto, Jpn. J. Appl. Phys., Part 1 **36**, 3924 (1997).

[7] A. Kumar, S. E. Laux, and F. Stern, Phys. Rev. B **42**, 5166 (1990).

[8] M. Fujito, A. Natori, and H. Yasunaga, Phys. Rev. B **53**, 9952 (1996).

[9] H. -M. Müller and S. E. Koonin, Phys. Rev. B **54**, 14 532 (1996).

[10] M. Macucci, K. Hess, and G. J. Iafrate, Phys. Rev. B **48**, 17 354 (1993); J. Appl. Phys. **77**, 3267 (1995); Phys. Rev. B **55**, 4879 (1997).

[11] M. Stopa, Phys. Rev. B **54**, 13 767 (1996).

[12] M. Koskinen, M. Manninen, and S. M. Reimann, Phys. Rev. Lett. **79**, 1389 (1997).

[13] S. Nagaraja, P. Matagne, V. Y. Thean, J. P. Leburton, Y. H. Kim, and R. M. Martin, Phys. Rev. B **56**, 15 752 (1997).

[14] I. H. Lee, V. Rao, R. M. Martin, and J. P. Leburton, Phys. Rev. B **57**, 9035 (1998).

[15] W. Kohn and L. J. Sham, Phys. Rev. **140**, A1133 (1965).

[16] For the exchange-correlation energy $\epsilon_{xc}(\mathbf{r})$, we use the parametrized form by Tanatar and Ceperley for the two-dimensional electron gas. B. Tanatar and D. M. Ceperley, Phys. Rev. B **39**, 5005 (1989).

[17] V. Shikin, S. Nazin, D. Heitmann, and T. Demel, Phys. Rev. B **43**, 11 903 (1991).

[18] T. Darnhofer and U. Rössler, Phys. Rev. B **47**, 16 020 (1993).

[19] We see no spin blockade phenomena (Ref. 20) for an elliptic potential, i.e., no jumps by more than spin 1/2. But we verify the spin blockade as found by Eto in the nonparabolic potential he considers. M. Eto, J. Phys. Soc. Jpn. **66**, 2244 (1997).

[20] D. Weinmann, W. Häusler, and B. Kramer, Phys. Rev. Lett. **74**, 984 (1995).